



## RESEARCH ARTICLE

# Combined endogenous MR biomarkers to assess changes in tumor oxygenation induced by an allosteric effector of hemoglobin

Thanh-Trang Cao-Pham<sup>1</sup> | An Tran-Ly-Binh<sup>1</sup> | Arne Heyerick<sup>2</sup> | Catherine Fillée<sup>3</sup> |  
Nicolas Joudiou<sup>1</sup> | Bernard Gallez<sup>1</sup>  | Bénédicte F. Jordan<sup>1</sup> 

<sup>1</sup>Louvain Drug Research Institute, Biomedical Magnetic Resonance Research Group, Université catholique de Louvain, Brussels, Belgium

<sup>2</sup>Normoxys Inc., Boston, Massachusetts

<sup>3</sup>Institut de Recherche Expérimentale et Clinique (IREC), UCLouvain, Université catholique de Louvain, Brussels, Belgium

## Correspondence

Bénédicte F. Jordan, Biomedical Magnetic Resonance Group (REMA), Louvain Drug Research Institute, UCLouvain, Université Catholique de Louvain, Avenue Mounier-B1.73.08, B-1200 Brussels, Belgium.  
Email: benedicte.jordan@uclouvain.be

## Funding information

Fournier-Majoie Foundation; Belgian National Fund for Scientific Research (FNRS)

Hypoxia is a crucial factor in cancer therapy, determining prognosis and the effectiveness of treatment. Although efforts are being made to develop methods for assessing tumor hypoxia, no markers of hypoxia are currently used in routine clinical practice. Recently, we showed that the combined endogenous MR biomarkers,  $R_1$  and  $R_2^*$ , which are sensitive to [dissolved  $O_2$ ] and [dHb], respectively, were able to detect changes in tumor oxygenation induced by a hyperoxic breathing challenge. In this study, we further validated the ability of the combined MR biomarkers to assess the change in tumor oxygenation induced by an allosteric effector of hemoglobin, *myo*-inositol trispyrophosphate (ITPP), on rat tumor models. ITPP induced an increase in tumor  $pO_2$ , as observed using L-band electron paramagnetic resonance oximetry, as well as an increase in both  $R_1$  and  $R_2^*$  MR parameters. The increase in  $R_1$  indicated an increase in  $[O_2]$ , whereas the increase in  $R_2^*$  resulted from an increase in  $O_2$  release from blood, inducing an increase in [dHb]. The impact of ITPP was then evaluated on factors that can influence tumor oxygenation, including tumor perfusion, saturation rate of hemoglobin, blood pH and oxygen consumption rate (OCR). ITPP decreased blood  $[HbO_2]$  and significantly increased blood acidity, which is also a factor that right-shifts the oxygen dissociation curve. No change in tumor perfusion was observed after ITPP treatment. Interestingly, ITPP decreased OCR in both tumor cell lines. In conclusion, ITPP increased tumor  $pO_2$  via a combined mechanism involving a decrease in OCR and an allosteric effect on hemoglobin that was further enhanced by a decrease in blood pH. MR biomarkers could assess the change in tumor oxygenation induced by ITPP. At the intra-tumoral level, a majority of tumor voxels were responsive to ITPP treatment in both of the models studied.

## KEYWORDS

magnetic resonance imaging, *myo*-inositol trispyrophosphate,  $\Delta R_1$ ,  $\Delta R_2^*$ , tumor hypoxia

**Abbreviations used:** DCE-MRI, dynamic contrast-enhanced MRI; dHb, deoxy-hemoglobin; EPR, electron paramagnetic resonance; ITPP, *myo*-inositol trispyrophosphate; MRI, magnetic resonance imaging; OCR, oxygen consumption rate; ODC, oxygen dissociation curve; ROI, region of interest

This is an open access article under the terms of the Creative Commons Attribution-NonCommercial-NoDerivs License, which permits use and distribution in any medium, provided the original work is properly cited, the use is non-commercial and no modifications or adaptations are made.

© 2019 The Authors. NMR in Biomedicine published by John Wiley & Sons Ltd

## 1 | INTRODUCTION

Hypoxia is a common situation occurring in solid tumors. A reduction in tumor oxygenation is the result of an insufficient oxygen supply and the increasing oxygen demand of tumor cells. Hypoxia is known to be a factor that can contribute to the failure of cancer treatment as well as to tumor recurrence.<sup>1</sup> One attractive strategy to improve the effectiveness of radiation therapy is to decrease hypoxia at the time of irradiation. A meta-analysis of over 10 000 patients from 86 randomized trials showed that modifying tumor hypoxia improved the outcome of patients treated with radiation therapy with an odds ratio of 0.77.<sup>2</sup> However, such an intervention only produced a modest benefit, as screening for the presence of hypoxia had not been an entry criterion prior to hypoxia modification in these trials. A better treatment response was observed in trials in which hypoxia was identified in tumors prior to irradiation. Thus, there is a growing need to detect hypoxic tumors and patients who could benefit from hypoxia modification. Various techniques have been developed to quantify tumor oxygenation, including <sup>19</sup>F-MRI of perfluorocarbon,<sup>3</sup> electron paramagnetic resonance (EPR) oximetry,<sup>4</sup> <sup>1</sup>H-MRI of hexamethyldisiloxane PISTOL,<sup>5</sup> PET imaging of nitroimidazoles,<sup>6</sup> <sup>19</sup>F MRI/MRS of fluorinated nitroimidazoles,<sup>7</sup> polarographic needle electrodes<sup>8</sup> and fiber optic probes.<sup>9</sup> However, so far no standard method has become available for routine clinical practice, as none of these techniques are currently able to address all of the practical challenges, such as noninvasiveness, tumor accessibility, or spatial and temporal resolutions.

Among the various oximetric techniques, imaging is regarded as an appropriate method for hypoxia detection because it is adapted to two observable features of hypoxia: spatial and temporal variations in oxygenation.<sup>10</sup> In order for an imaging technique to be adopted in routine oncology practice, a number of requirements need to be met, such as noninvasiveness, the possibility of repeated measurements, high spatial and temporal resolution, cost-effectiveness, robustness and easy translation to human trials.<sup>10</sup> One potential method to evaluate tumor hypoxia consists of the assessment of the oxygen-sensitive endogenous MR contrast parameters,  $R_1$  and  $R_2^*$ , which fulfills most of these criteria. Both MR biomarkers are sensitive to the change in  $pO_2$ , but reflect distinct features. The dissolved paramagnetic molecular oxygen in tissue fluid and in blood plasma increases the spin lattice relaxation rate  $R_1$  via dipolar interaction. Meanwhile, the effective spin-spin relaxation rate  $R_2^*$  is accelerated by an increase in paramagnetic deoxyhemoglobin. Because dissolved  $O_2$  is mainly present in tissue while dHb exists only in blood vessels,  $R_1$  primarily reflects tissue oxygenation while  $R_2^*$  is more sensitive to changes in blood oxygenation.<sup>10-14</sup>

One drawback of  $R_1$  is its low sensitivity. Starting from the fact that the solubility of oxygen is better in lipids than in water, our group previously assessed the signal of  $R_1$  of lipid protons ( $R_{1L}$ ) instead of the global  $R_1$  ( $R_{1G}$ ) (which mostly reflects the signal of water protons [ $R_{1W}$ ]), expecting that it should be more sensitive to the changes in  $pO_2$ .<sup>15,16</sup>

It should be noted that a change in tumor  $pO_2$  is the additive result of multifactorial processes within the tumor. Each technique can only provide information about one or more facets of the overall change in the tumor microenvironment. Thus, there is an interest in combining multiple parameters to expand the understanding and assessment of tumor hemodynamics, which are essential for personalized treatment. In a previous study, we combined  $R_1$  and  $R_2^*$  to evaluate the changes in tumor  $pO_2$  induced by a hyperoxic gas breathing challenge.<sup>14</sup>

The aim of the current study was to further validate the combined endogenous MRI contrast parameters  $R_1$  (including  $R_{1G}$ ,  $R_{1W}$  and  $R_{1L}$ ) and  $R_2^*$  to assess the change in tumor oxygenation. For this purpose, we used another oxygen modifier, with a different mechanism of action from the hyperoxic gas breathing challenge. Tumor  $pO_2$  can be improved by manipulating the oxygen unloading capacity of blood. The allosteric effector of hemoglobin promotes the dissociation of oxygen from hemoglobin by right-shifting the oxygen dissociation curve, thus increasing tumor oxygenation. Compounds under clinical investigation such as OXY111A (myo-inositol trispyrophosphate [ITPP]) (<http://normoxys.com/clinical-trial-results/>) and Efaproxiral<sup>17</sup> were well tolerated and induced an increase in partial pressure of oxygen in preclinical models. Efaproxiral has reached phase III in patients with brain metastases from breast cancer. However, no significant improvement in overall survival has been observed using the combination of Efaproxiral and whole brain radiation therapy.<sup>18</sup> In this context, we chose ITPP to induce change in tumor  $pO_2$ .<sup>19-21</sup> The compound has been found to decrease hypoxia and improve tumor outcome in various animal models when used as a monotherapy or combined with chemotherapy.<sup>22-24</sup> The phase I clinical investigation showed a good tolerance of patients to ITPP.<sup>19</sup>

## 2 | MATERIALS AND METHODS

The study was approved by the local ethics committee. Studies were undertaken in accordance with the national and local regulations of the ethics committee (agreement number UCL/2014/MD/026).

### 2.1 | Tumor models

Two tumor models were included in the study: rhabdomyosarcoma and 9 L-glioma. Rhabdomyosarcoma cells were grown in Roswell Park Memorial Institute (RPMI) medium supplemented with 10% fetal calf serum (heat inactivated), and a 1% mixture of antibiotics (penicillin 100 UI/mL, streptomycin 0.1 mg/mL) for in vitro experimentation. For in vivo study, fragments from a syngeneic rhabdomyosarcoma (1 mm<sup>3</sup>) were grafted subcutaneously into one thigh of male adult WAG/Rij rats. The model was developed by the Laboratory of Experimental Radiobiology, Katholieke

Universiteit Leuven, Belgium. 9 L-glioma cells were grown in RPMI medium supplemented with 10% fetal calf serum (heat inactivated), a 1% mixture of antibiotics (penicillin 100 UI/mL, streptomycin 0.1 mg/mL), 1% nonessential amino acids and 1% sodium pyruvate. To establish 9 L-glioma tumors in vivo, male adult Fisher F344 rats were inoculated subcutaneously in their thighs with  $5 \times 10^6$  cells. Tumor implantations were performed on the rats under general anesthesia with intraperitoneal (IP) injection of ketamine and xylazine (80 and 10 mg/kg, respectively) on rats weighing between 200 and 250 g. The animals were introduced into the study when the tumors reached the size of 15 to 20 mm.

## 2.2 | ITPP treatment

ITPP was generously provided by NormOxys Inc. (Boston, MA). For in vivo study, ITPP was prepared at a concentration of 200 mg/mL in saline for IP injection at a dose of 2 g/kg. For in vitro study, adherent cells were treated with medium containing 10mM ITPP. The effect of ITPP was studied after 2 hours of treatment.

## 2.3 | In vivo experimental design

Four cohorts were involved:

- Tumor  $pO_2$  was measured on nine rhabdomyosarcomas and 10 9 L-gliomas.
- The MRI measurements were performed on eight rhabdomyosarcomas and nine 9 L-gliomas.
- The blood gas test for the measurement of the saturation of hemoglobin and of blood pH was performed on five healthy Fischer rats.
- 20 rhabdomyosarcomas and 14 9 L-gliomas were used for the measurement of the perfused area by the Patent Blue staining method.

For tumor  $pO_2$  and perfusion measurement studies, animals were allocated to two groups: vehicle (NaCl 0.9%) and ITPP. For MRI and blood gas test studies, animals were measured at two time points: before and 2 hours after ITPP treatment.

## 2.4 | L-band EPR oximetry

L-band EPR spectroscopy allowed the direct measurement of tumor oxygenation through the conversion of EPR linewidth to  $pO_2$  using a calibration curve.<sup>25</sup> Briefly, charcoal wood powder (CX0670-1, EM Science, Gibbstown, NJ) was used as an oxygen-sensitive sensor. About 200  $\mu$ L of charcoal suspension (100 mg/mL) was introduced within the tumor at a depth of 3–6 mm using a 23-gauge needle. EPR experiments were performed 24 hours after probe implantation using an L-band EPR spectrometer (Magnetech, Berlin, Germany) equipped with a low-frequency microwave bridge operating at 1.2 GHz and a loop-gap resonator. The animals were anesthetized (1.5% isoflurane, 2 L/min) for EPR measurement and the tumors were placed at the center of the loop-gap resonator, whose sensitivity extended to 1 cm around the loop. The modulation frequency was 100 kHz and the amplitude modulation was less than one third of the peak-to-peak linewidth to avoid peak distortion. The linewidth of the first-derivative EPR spectrum that was the average of five scan accumulations was then converted to  $pO_2$  using a calibration curve. After the baseline  $pO_2$  value had been recorded, the animals were treated with ITPP (six 9 L-gliomas, three rhabdomyosarcomas) or NaCl 0.9% (four 9 L-gliomas, six rhabdomyosarcomas) and image acquisition was then repeated after 2 hours of administration.

## 2.5 | Blood gas test

Venous blood samples were taken from the animals at two time points: before and 2 hours after ITPP administration. The rats were anesthetized with 1.5% isoflurane during blood sampling. Gas delivery (medical air containing 21%  $O_2$  mixed with isoflurane) was continuous at 2 L/min through a nosepiece. About 1 mL of blood was drawn from the lateral tail vein to a special blood test syringe (safePICO Aspirator, Radiometer Medical, Denmark). The gas bubble was removed and the blood was kept from exposure to the external air thanks to a special cap. The sample was mixed with heparin present in the syringe to reduce the risk of clots. Blood samples were analyzed by an ABL901 analyzer (Radiometer, Denmark) within 1 hour after sampling.

## 2.6 | MRI study

The rats were anesthetized with 1.5% isoflurane (2 L/min) during the MRI experiments. MRI measurements were made before and 2 hours after ITPP administration.

In order to compare the effect of ITPP treatment on the voxel scale, the animals were monitored longitudinally over time to acquire individual data in the pretreatment and posttreatment conditions. For this purpose, temperature and breathing rate were monitored using MR-compatible

probes throughout the image acquisition process. Temperature was kept constant using a water-circulating blanket connected to a heated water bath.

MRI was performed on an 11.7 T, 16 cm inner diameter bore system (Bruker, Biospec) with a 7 cm diameter birdcage coil for signal transmission and a surface array coil (2 x 2 elements, 18 x 18 mm<sup>2</sup> each) for signal reception. A warm water blanket was used to maintain the animals' temperature at 37°C, and the temperature was monitored with an MR-compatible rectal probe.

A multislice Rapid Acquisition with Relaxation Enhancement (RARE) sequence was first used to determine the most representative tumor slice for further measurement, with the following parameters: TE/TR/RARE-factor/FOV/matrix size/slice thickness = 10.66 ms/2500 ms/6/35 x 35 mm/256 x 256/1 mm. The representative slice was selected manually for each tumor. It was typically the largest slice of each tumor. The segmented IR-FISP sequence (SSFP-FID mode) was used for R<sub>1</sub> acquisition with the following parameters: TR/TE/FA/BW/FOV/matrix size/slice thickness = 4 ms/1.35 ms/10°/100 kHz/55 x 30 mm/100 x 85/1 mm, four segments, 100 TI from 13 ms to 8329 ms every 84 ms, and a total acquisition time of 20 minutes. The resonant frequency for excitation of R<sub>1</sub> sequence was set at the resonance of water. Multi-Gradient Echo R<sub>2</sub>\* images were acquired at TR/FA/slice thickness = 3000 ms/15°/1 mm with a FOV of 35 x 35 mm on a 256 x 256 matrix, with 12 echoes from 3.5 to 58.5 ms every 5 ms. The total acquisition time was 9 minutes 36 seconds.

Data analysis was performed with an in-house program developed in ImageJ and MATLAB (MATLAB R2013b, The Math Works). R<sub>1</sub> and R<sub>2</sub>\* maps were calculated with an MRI analysis calculator plug-in in ImageJ software. This MRI analysis method is adapted from the original plug-in created by Karl Schmidt (<http://rsb.info.nih.gov/ij/>) using a curve-fitting method based on the Simplex method. R<sub>1L</sub> and R<sub>1W</sub> were extracted from the R<sub>1G</sub> map by a bi-exponential deconvolution method. Hence, the term R<sub>1G</sub> refers to the R<sub>1</sub> acquired by MRI and is the sum of the contributors of R<sub>1W</sub> and R<sub>1L</sub>. Meanwhile, R<sub>1L</sub> and R<sub>1W</sub> indicate the generated data obtained by the deconvolution of R<sub>1G</sub>. Regions of interest (ROIs) were drawn manually around the tumor on the selected anatomic slice and were transferred to R<sub>1L</sub>, R<sub>1W</sub>, R<sub>1G</sub> and R<sub>2</sub>\* maps of the same slice. The subtraction of the two maps acquired before and after ITPP treatment was performed voxel by voxel, resulting in maps of ΔR<sub>1L</sub>, ΔR<sub>1W</sub>, ΔR<sub>1G</sub> and ΔR<sub>2</sub>\*. Coregistration was performed using a homemade script on Matlab. During acquisition, similar orientation was used for the R<sub>2</sub>\* map and the R<sub>1</sub> map, so that only translation transformations were needed for coregistration.

## 2.7 | Perfusion study – Patent Blue staining

We used the Patent Blue staining method in order to obtain a rough estimate of the tumor perfusion fraction. This method has been validated by comparison with DCE-MRI.<sup>26,27</sup> Animals were treated with vehicle, 1 mL NaCl 0.9% (10 rhabdomyosarcomas and six 9 L-gliomas), or ITPP (10 rhabdomyosarcomas and eight 9 L-gliomas). Two hours after treatment, Patent Blue was injected through the tail vein (Sigma-Aldrich, 1 mL of Patent Blue solution 1.25%). The animals were sacrificed by an overdose of pentobarbital exactly 1 minute after the administration of Patent Blue. The tumors were rapidly excised and cut into two size-matched halves. Pictures of each tumor cross section were taken with a digital camera. The tumor perfusion fraction was estimated as the percentage of stained area of the whole tumor cross section analyzed by ImageJ.

## 2.8 | Oxygen consumption rate

The oxygen consumption rate (OCR) was measured in vitro using a Bruker EMXplus EPR spectrometer operating at 9.5 GHz. Briefly, adherent cells were trypsinized and resuspended in fresh medium (10<sup>7</sup> cells/mL). A mix of 100 μL of cell suspension and 100 μL of 20% dextran was sealed in a glass capillary tube in the presence of 0.2mM of a nitroxide probe acting as an oxygen sensor (<sup>15</sup>N 4-oxo-2,2,6,6-tetramethylpiperidine-d<sub>16</sub>-<sup>15</sup>N-1-oxyl, CDN isotopes, Pointe-Claire, Quebec, Canada). The sample was placed in a quartz ESR tube and maintained at 37°C by heated nitrogen during the acquisition of the spectra. EPR linewidth was measured every minute and reported on a calibration curve to obtain the oxygen concentration.<sup>28</sup> OCR was determined by the absolute value of the slope of the decrease in oxygen concentration in the closed capillary tube over time.

## 2.9 | Statistical analysis

Statistical analyses were performed with the GraphPad (Prism) program. Results were expressed as mean ± SEM (standard error of the mean). To evaluate the differences between groups of data, we used the two-tailed t-test. For all tests, *P* < 0.05 was regarded as significant (\**P* < 0.05; \*\**P* < 0.01; \*\*\**P* < 0.001; \*\*\*\**P* < 0.0001).

## 3 | RESULTS

In a preliminary study, tumor pO<sub>2</sub> in rhabdomyosarcomas and in 9 L-gliomas was monitored longitudinally by EPR oximetry.<sup>29</sup> We found that a single dose of ITPP induced an increase in tumor pO<sub>2</sub> that was maximal at 2 hours postadministration.<sup>29</sup> In this study, we selected this time point to evaluate the impact of ITPP treatment on tumor pO<sub>2</sub> and oxygen-dependent MR parameters in two rat tumor models.



The change in in vivo tumor  $pO_2$  was confirmed by L-band EPR oximetry (Figure 1, Table 1). In both models under study, we did not notice any change in tumor  $pO_2$  in the control group before and 2 hours after saline administration. However, we observed that ITPP treatment significantly increased tumor  $pO_2$  in both models ( $P < 0.01$ ) at the same time point. The change (0- vs. 2-h ITPP) was significantly greater in 9 L-gliomas than in rhabdomyosarcomas ( $P < 0.01$ , Table 1B).

Figures 2 and 3 present pre- and post-ITPP treatment MRI data for rhabdomyosarcomas and 9 L-gliomas, respectively. The data were normalized to the baseline values. The reproducibility of  $R_1$  and  $R_2^*$  measurements in the two tumor models is reported in Table 2.

A change in  $R_2^*$  may be due to a change in [dHb] per volume of tissue, which possibly relates to the change in  $O_2$  released from the blood. ITPP significantly increased  $R_2^*$  from  $83.8 \pm 6.4$  to  $98.6 \pm 8.7 \text{ s}^{-1}$  in rhabdomyosarcomas ( $P < 0.01$ , Figure 2A) and from  $83.1 \pm 4.3$  to  $89.6 \pm 4.4 \text{ s}^{-1}$  in 9 L-gliomas ( $P = 0.02$ , Figure 3A).  $R_2^*$  of all tumors in both models studied ( $n = 8\text{-}9/\text{model}$ ) increased after ITPP administration, except for one 9L-glioma tumor, which showed a decrease in  $R_2^*$  (Figure 3A).

A change in  $R_1$  could be the result of a change in dissolved  $O_2$ . A significantly faster relaxation rate was generally observed for all  $R_1$  parameters ( $R_{1G}$ ,  $R_{1W}$  and  $R_{1L}$ ) in both models after ITPP administration ( $P < 0.05$ ) (Figures 2 and 3B-D).  $R_{1G}$  increased from  $2.11 \pm 0.03$  to  $2.19 \pm 0.04 \text{ s}^{-1}$  in rhabdomyosarcomas ( $P < 0.01$ , Figure 2B) and from  $2.12 \pm 0.05$  to  $2.25 \pm 0.05 \text{ s}^{-1}$  in 9 L-gliomas ( $P = 0.05$ , Figure 3B).  $R_{1W}$  was  $1.01 \pm 0.01 \text{ s}^{-1}$  (vehicle) and  $1.08 \pm 0.02 \text{ s}^{-1}$  (ITPP) ( $P < 0.01$ ) in rhabdomyosarcomas (Figure 2C) and  $1.05 \pm 0.01 \text{ s}^{-1}$  (vehicle) and  $1.13 \pm 0.02 \text{ s}^{-1}$  (ITPP) ( $P < 0.01$ ) in 9 L-gliomas (Figure 3C).  $R_{1G}$  increased after ITPP treatment in both tumor models (Figures 2B and 3B). However, for the  $R_{1W}$  parameter, there was one tumor in each model presenting an opposite trend in response to ITPP treatment. In response to ITPP,  $R_{1L}$  increased from  $3.24 \pm 0.08$  to  $3.36 \pm 0.09 \text{ s}^{-1}$  ( $P = 0.04$ ) (Figure 2D) and from  $3.45 \pm 0.06$  to  $3.57 \pm 0.07 \text{ s}^{-1}$  ( $P < 0.01$ ) (Figure 3D) in rhabdomyosarcomas and 9 L-gliomas, respectively. Two rhabdomyosarcomas and one 9 L-glioma showed a decrease in  $R_{1L}$  after ITPP treatment.  $R_{1L}$  was not shown to be more sensitive to changes in tumor oxygenation than  $R_{1G}$  or  $R_{1W}$  in these models.

Figure 4 shows representative anatomic images as well as the  $\Delta R_1$  and  $\Delta R_2^*$  maps of one 9 L-glioma and one rhabdomyosarcoma. Figure 5 shows the heterogeneity in  $R_1$  and  $R_2^*$  response to ITPP challenge in rhabdomyosarcomas and in 9 L-gliomas at the inter-tumoral level. In both models, ITPP induced increases in  $R_1$  and  $R_2^*$  in most (>50%) of the voxels in each tumor.

Since  $R_2^*$  is sensitive to the change in [dHb], we assessed the impact of ITPP on  $HbO_2$  saturation in the blood (Figure 6). ITPP significantly decreased the saturation of hemoglobin from  $91.6 \pm 1.1\%$  to  $67.9 \pm 4.4\%$  ( $P < 0.01$ ) (Figure 6A). Interestingly, we also found a slight but significant

**FIGURE 1** Tumor oxygenation of (A) rhabdomyosarcomas (vehicle  $N = 6$ , *myo*-inositol trispyrophosphate [ITPP]  $N = 3$ ) and (B) 9 L-gliomas (vehicle  $N = 4$ , ITPP  $N = 6$ ) obtained by L-band electron paramagnetic resonance (EPR) oximetry before and 2 hours after ITPP or saline administration (mean  $\pm$  SEM). Both tumor models were responsive to ITPP, with a significant increase in tumor  $pO_2$ . Saline injection did not change tumor  $pO_2$ . \*\* $p < 0.01$ , \*\*\* $p < 0.001$ , \*\*\*\* $p < 0.0001$ , ns = not significant

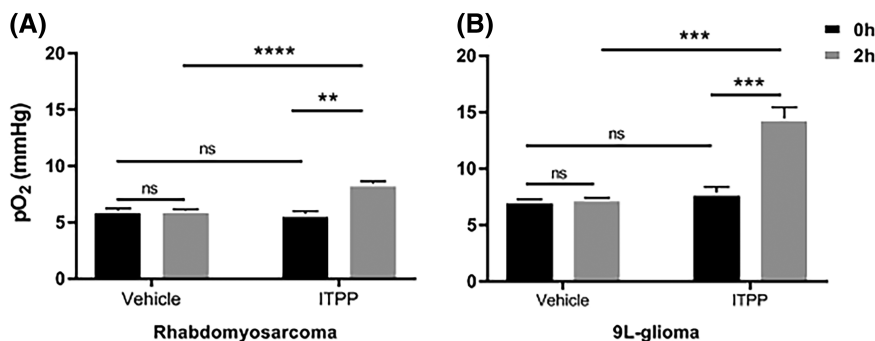


**TABLE 1** Summary of (A) tumor  $pO_2$  (mmHg) assessed by electron paramagnetic resonance (EPR) band L in vehicle- and *myo*-inositol trispyrophosphate (ITPP)-treated tumors and (B) the change in tumor  $pO_2$  induced by ITPP compared with the vehicle group (2-hour vehicle) and pretreatment group (0-hour ITPP). (Mean  $\pm$  SEM)

	Vehicle (mmHg)		ITPP (mmHg)		
	0 h	2 h	0 h	2 h	
(A)					
Rhabdomyosarcoma	6 $\pm$ 0.2	6 $\pm$ 0.1	5.7 $\pm$ 0.3	8.4 $\pm$ 0.1	
9 L-glioma	7.2 $\pm$ 0.1	7.3 $\pm$ 0.1	7.8 $\pm$ 0.5	14.4 $\pm$ 1	
	0-h ITPP vs. 2-h ITPP (mmHg)		2-h vehicle vs. 2-h ITPP (mmHg)		T-test
(B)					
Rhabdomyosarcoma					$P > 0.05$
9 L-glioma					$P > 0.05$
T-test	$P < 0.01$		-		

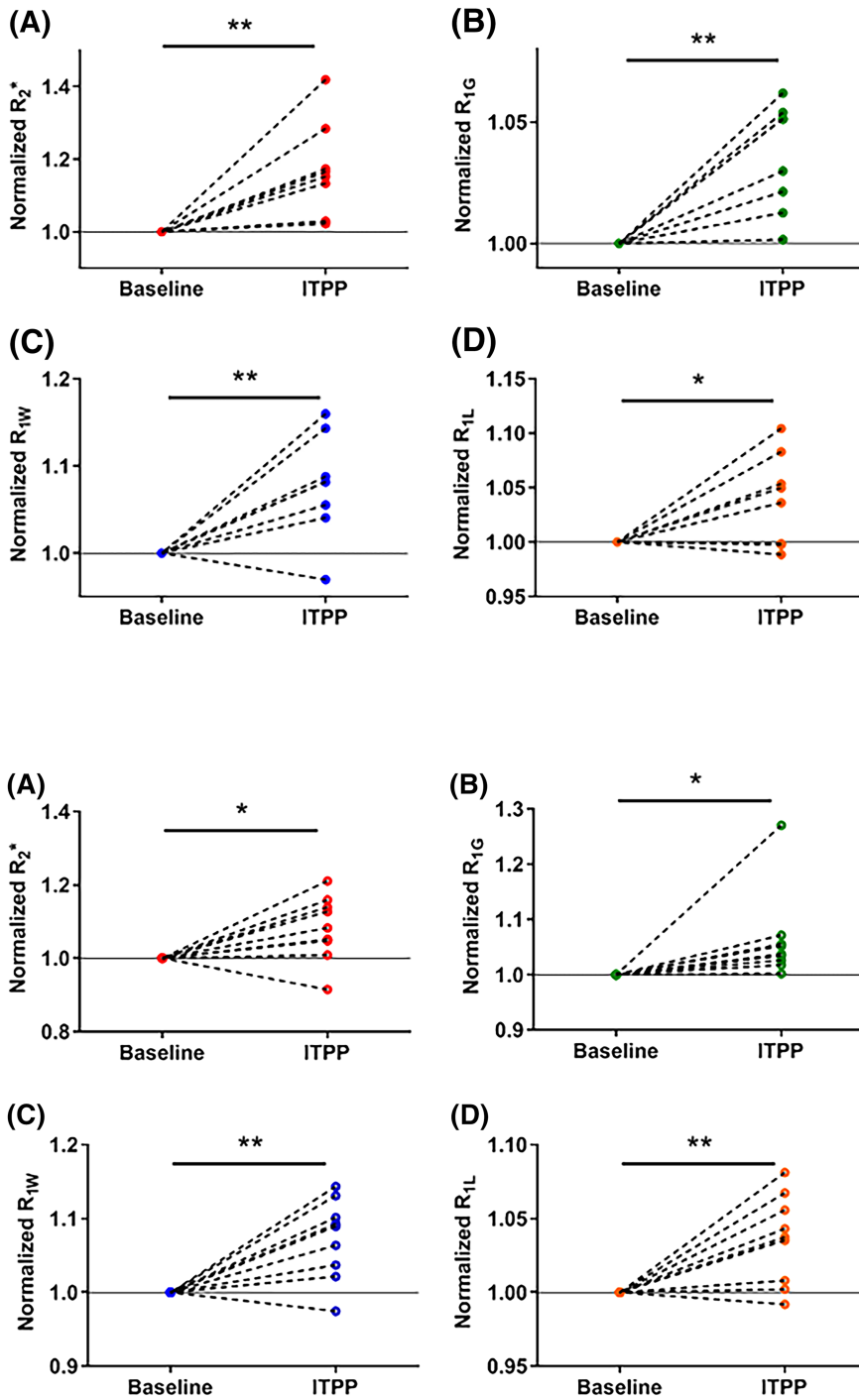


**FIGURE 2** Individual normalized changes in magnetic resonance imaging (MRI) parameters in rhabdomyosarcomas ( $N = 8$ ) before and 2 hours after *myo*-inositol trispyrophosphate (ITPP) administration. All MRI parameters increased under the effect of ITPP \* $p < 0.05$ , \*\* $p < 0.01$

**FIGURE 3** Individual normalized changes in magnetic resonance imaging (MRI) parameters in 9 L-gliomas ( $N = 9$ ) before and 2 hours after *myo*-inositol trispyrophosphate (ITPP) administration. All MRI parameters increased under the effect of ITPP \* $p < 0.05$ , \*\* $p < 0.01$

**TABLE 2** Coefficient of variation (COV) of  $R_1$  and  $R_2^*$  measurements in 9 L-gliomas and in rhabdomyosarcomas. Each COV value was calculated for the corresponding data set. The previous presentation may induce confusion. Thus, we have added the % after each COV value

	Rhabdomyosarcoma		9 L-glioma	
	Baseline	ITPP	Baseline	ITPP
$R_2^*$	21.7%	25%	15.7%	14.8%
$R_{1G}$	4.2%	4.8%	7.7%	6%
$R_{1W}$	2.4%	3.9%	3.3%	5.6%
$R_{1L}$	6.8%	7.8%	5.2%	5.9%

decrease in blood pH: the pH values were  $7.46 \pm 0.01$  and  $7.40 \pm 0.01$  for the vehicle- and ITPP-treated samples, respectively ( $P < 0.01$ , paired t-test) (Figure 6B). Both factors can contribute to a right-shift of the oxygen dissociation curve (ODC).

We further tested the impact of ITPP on the perfusion of tumors to verify whether the change in  $R_2^*$  might be due to a change in tumor perfusion. The Patent Blue staining method provides a rough estimation of the tumor-perfused fraction.<sup>26,27</sup> The experiment showed no difference in the percentage of colored area between tumors in the vehicle group and tumors treated with ITPP in either model (Figure 7). The colored area percentages were  $82.5 \pm 2.7\%$  (vehicle,  $n = 10$ ) and  $77.2 \pm 2.1\%$  (ITPP,  $n = 10$ ) ( $P = 0.14$ ) for rhabdomyosarcomas and  $56.7 \pm 2.5\%$  (vehicle,  $n = 6$ ) and  $44.0 \pm 4.9\%$  (ITPP,  $n = 8$ ) ( $P = 0.06$ ) for 9 L-gliomas. We excluded the potential role of an increase in  $R_2^*$  related to a change in perfusion. It should be noted that rhabdomyosarcomas were better perfused than 9 L-gliomas ( $P < 0.01$ , unpaired t-test).

Two factors determine tumor  $pO_2$ :  $O_2$  supply and  $O_2$  consumption of tumor cells. An increase in tumor  $pO_2$  can be induced by increasing the  $O_2$  supply and/or decreasing the  $O_2$  consumption. The in vitro OCR of both cell lines was assessed by X-band EPR oximetry and the results are presented in Figure 8. ITPP treatment significantly decreased OCR in both cell lines. OCR decreased from  $15.21 \pm 0.5$  to  $7.85 \pm 0.51$   $\text{nmol } O_2/\text{min}/5 \times 10^6$  cells ( $P < 0.01$ ) and from  $7.47 \pm 0.61$  to  $5.3 \pm 0.43$   $\text{nmol } O_2/\text{min}/5 \times 10^6$  cells ( $P = 0.02$ ) for rhabdomyosarcoma and 9L-glioma cells, respectively.

## 4 | DISCUSSION

In a previous study, we highlighted the added value of combining  $R_1$  and  $R_2^*$  MRI biomarkers to map changes in tumor oxygenation induced by a hyperoxic breathing challenge.<sup>14</sup>  $R_1$  and  $R_2^*$  were successfully integrated in a single map to visualize four different types of voxels corresponding

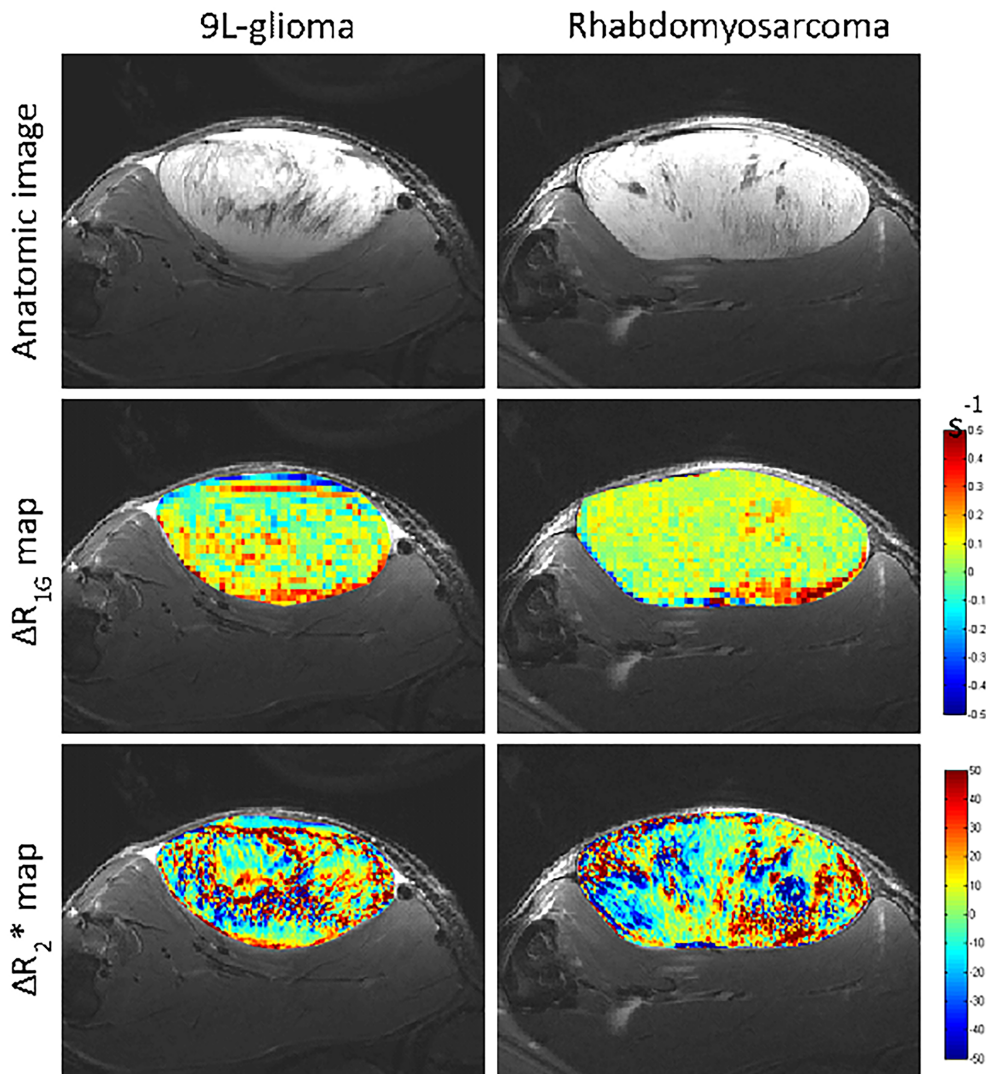


**FIGURE 4** Representative anatomic images,  $\Delta R_1$  maps and  $\Delta R_2^*$  maps of a 9 L-glioma and a rhabdomyosarcoma. The delta maps were obtained by subtracting the baseline maps from post-*myo*-inositol trispyrophosphate (ITPP) treatment maps

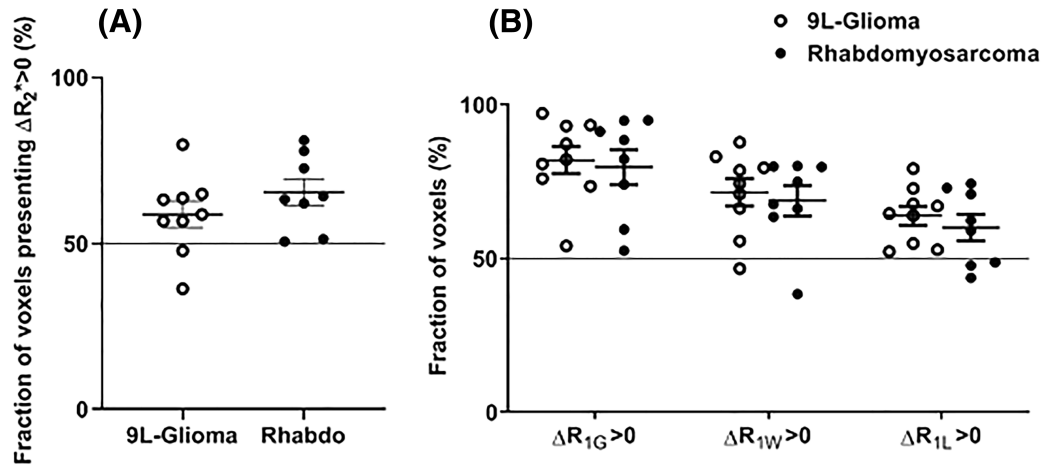


**FIGURE 5** Mean fractional myo-inositol trispyrophosphate (ITPP)-induced (A)  $\Delta R_2^* > 0$  and (B)  $\Delta R_1 > 0$  of rhabdomyosarcomas (filled circles) and 9 L-gliomas (open circles) (mean  $\pm$  SEM). Each symbol presents the data of a tumor. At the intra-tumor level, a majority of voxels in most of the tumors presented  $\Delta R_1 > 0$  and  $\Delta R_2^* > 0$

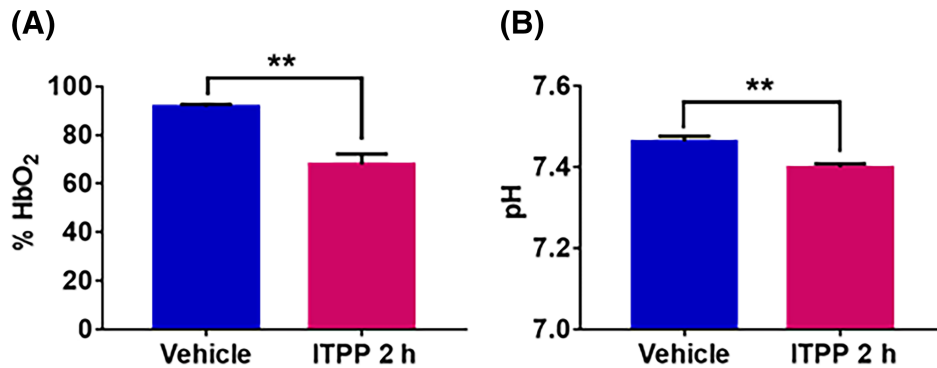


**FIGURE 6** (A) Change in hemoglobin saturation before and 2 hours after myo-inositol trispyrophosphate (ITPP) administration in healthy venous rat blood sample ( $N = 5$ ). ITPP significantly decreases the rate of hemoglobin saturation (mean  $\pm$  SEM). (B) Change in venous blood pH before and 2 hours after ITPP administration in healthy venous rat blood sample ( $N = 5$ ). ITPP slightly but significantly decreases the blood pH (mean  $\pm$  SEM) \*\* $p < 0.01$

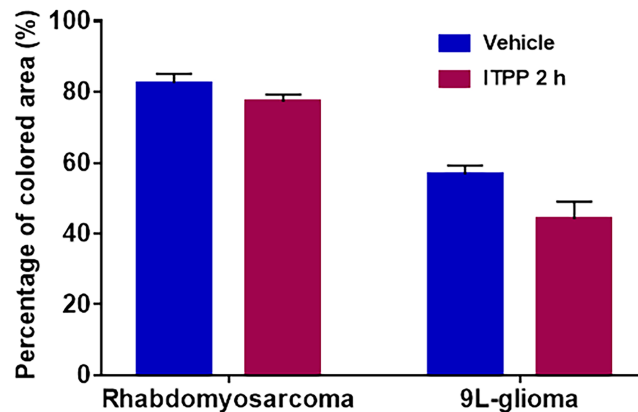


**FIGURE 7** Mean value  $\pm$  SEM of Patent Blue-perfused area in rhabdomyosarcomas (vehicle  $N = 10$ ; myo-inositol trispyrophosphate [ITPP]  $N = 10$ ) and in 9 L-gliomas (vehicle  $N = 6$ ; ITPP  $N = 8$ ). No significant difference was observed between the vehicle group and the group treated with ITPP in either model

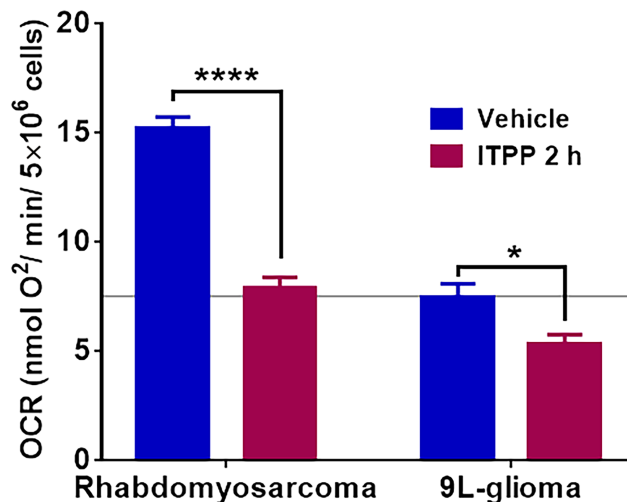


**FIGURE 8** Impact of *myo*-inositol trispyrophosphate (ITPP) on in vitro oxygen consumption rate (OCR) in rhabdomyosarcoma cell line (vehicle N = 6; ITPP N = 6) and in 9 L-glioma cell line (vehicle N = 8; ITPP N = 6) obtained by X-band electron paramagnetic resonance (EPR) oximetry. ITPP significantly decreased the OCR in both tumor cell lines (mean  $\pm$  SEM) \* $p < 0.05$ , \*\*\*\* $p > 0.0001$

to different hypoxic tumor regions.<sup>14</sup> In the current study, we further validated the value of the combined  $R_1$  and  $R_2^*$  MR oxygen-dependent parameters for assessing changes in tumor oxygenation induced by a pharmacological oxygen modifier agent, ITPP, which is described as right-shifting the dissociation curve of Hb-O<sub>2</sub> towards higher  $pO_2$  values.<sup>30</sup>

All oxygen-sensitive MR parameters ( $R_{1G}$ ,  $R_{1W}$ ,  $R_{1L}$  and  $R_2^*$ ) increased after ITPP administration (Figures 2 and 3). The result at the inter-tumoral level was confirmed at the intra-tumoral level (Figure 5), as the majority of tumors in both models presented a higher proportion of voxels with ITPP-induced  $\Delta R_1 > 0$  or  $\Delta R_2^* > 0$ . We also found that  $R_{1L}$  and  $R_{1W}$  did not show any superiority to  $R_{1G}$  in terms of sensitivity to the change in tumor oxygenation induced by ITPP. We even observed a higher fractional increase in  $R_{1W}$  (~ 8%) than in  $R_{1L}$  (~ 3.5%) after ITPP administration in both tumor models. A possible explanation for this may lie in the method used to extract the  $R_{1L}$  and  $R_{1W}$  values from  $R_{1G}$ . The bi-exponential method is a model that attributes the fast and slow components to lipid and water proton relaxation rates, respectively. However, this approximation cannot exclude the potential contribution to the fast component of the relaxation of water linked to macromolecules. Thus, the fast component does not exclusively reflect lipid relaxation. However, the observation is consistent with that obtained in previous studies using a hyperoxic breathing challenge (carbogen).<sup>14,15</sup> It should also be noted that, despite the higher fractional increase observed in  $R_{1W}$  than in  $R_{1L}$ , the absolute change in  $R_1$  was higher in  $R_{1L}$  than in  $R_{1W}$  (approximately 0.07 and 0.12 for  $R_{1W}$  and  $R_{1L}$ , respectively).

Recently,  $R_1$  has attracted more and more attention as a tool for estimating tumor oxygenation, as it is directly sensitive to dissolved O<sub>2</sub> concentration. An increase in  $R_1$  is generally observed in tumors under hyperoxic challenge.<sup>11,13,15,31</sup> O'Connor et al have validated the mapping of spatial variation of hypoxia based on the different response of  $R_1$  to oxygen breathing.<sup>12</sup> Because  $R_1$  is sensitive to the oxygen molecules dissolved in plasma and tissue fluid, the increase in  $R_1$  corresponds to an increase in dissolved oxygen in tumor tissue. With respect to changes in oxygenation, two mechanisms may be involved in the modification of tumor oxygenation: an increase in the O<sub>2</sub> supply and a decrease in the OCR of tumor cells. While an increase in O<sub>2</sub> supply by right-shifting the ODC of ITPP was previously shown,<sup>19-21</sup> we have demonstrated here that ITPP was also able to induce a significant reduction of OCR in vitro, in both tumor cell lines studied. Previously, evidence showed that ITPP was able to inhibit the PI3K pathway.<sup>22</sup> This mechanism could explain the decrease in OCR induced by ITPP.<sup>32,33</sup> The effect of ITPP in reducing cell OCR was compared with an inhibitor of PI3K, LY294002.<sup>29</sup> Both ITPP and LY294002 reduced OCR of 9 L-glioma and rhabdomyosarcoma cell lines with the same timing.<sup>29</sup> Interestingly, the fraction of tumor with  $\Delta R_1 > 0$  is highly variable, ranging from less than 50% to almost 100%. Two factors may contribute to this intra-tumor heterogeneity of  $R_1$  response. First, the distribution of ITPP relies on the tumor vascular system. The chaotic, disorganized structure of tumor vessels may hinder the accessibility of the compound to regions where the blood supply is reduced. Consequently, a tumor's heterogeneous vessel architecture determines drug uptake in its different regions. Second, the magnitude of response to ITPP depends on the tissue's oxygenation at baseline.

An increase in  $R_2^*$  is the result of an increase in the paramagnetic Hb concentration per tissue volume. The ability of ITPP to change the Hb saturation was assessed in vivo on venous blood in healthy rats. In addition, ITPP also slightly but significantly increased blood acidity. Both factors therefore contributed to a right-shift of ODC towards a higher O<sub>2</sub> release from the blood and an increase in the total dHb content according to the Bohr effect. We also compared the perfusion in treated and untreated tumors to evaluate whether ITPP could induce an acute effect on tumor perfusion, which in turn could modify the tumor blood volume and dHb content. Our study did not show any significant change in tumor perfusion after ITPP administration. It should be noted that Kieda et al<sup>22</sup> found that long-term ITPP treatment in melanoma and in breast cancer synergic

models was able to normalize tumor vessels through the acquisition of a matured phenotype in endothelial cells and the reorganization of the tumor vessels. However, this effect did not occur soon (2 hours) after ITPP administration in our study (Figure 7).

In this study, the field strength of the MRI was 11.7 T, which is much stronger than the 1.5 and 3 T MR clinical systems used in clinical practice. In the study of Blockley et al,<sup>33</sup> the authors measured  $R_2^*$  versus Hb concentration at 1.5, 3 and 7 T. They demonstrated that the transverse relaxivity ( $R_2^*$ ) of whole blood as a function of dHb concentration (in  $s^{-1}mM^{-1}$ ) increased as the magnetic field strength increased. We can speculate that the  $R_2^*$  measured in this study at a high field strength is more sensitive to the change in dHb content than the measurements reported at a lower field strength.

Finally, with respect to  $R_2^*$  measurement, we used a low flip angle ( $10^\circ$ ) to minimize any potential "in-flow" effect,<sup>34</sup> as the signal created by the water blood flowing into the imaging slice is much stronger than the static water at high flip angles ( $30^\circ$ - $90^\circ$ ) because the spin of the static water is partially saturated by previous pulses.

While  $R_2^*$  is generally assumed to decrease in response to a hyperoxic challenge, because the breathing of high oxygen content gas (carbogen or 100% oxygen) increases the hemoglobin saturation of blood and therefore decreases the  $R_2^*$  signal, we have shown here that the direction of change in  $R_2^*$  depends on the mechanism of action of the oxygen modifier under study. When a pharmacological agent is used that is able to modify Hb saturation and oxygen consumption, an increase in  $R_2^*$  is observed. This is similar to observations made using inhibitors of oxygen consumption.<sup>35</sup> Moreover, in a previous study, we showed that the change in  $R_2^*$  is influenced not only by tumor  $pO_2$  but also by the degree of Hb saturation at baseline.<sup>14</sup> This has also been proved at the intra-tumoral level in a study by Little et al.<sup>36</sup>

Interestingly, we observed that the better-oxygenated tumor model 9 L-glioma showed a higher increase in  $pO_2$  after ITPP administration compared with the rhabdomyosarcoma model (Figure 1), as the right-shift of the ODC will only be beneficial to tissues within a certain range of  $pO_2$  ("middle range", ie, 40–80 mmHg) and ITPP will barely affect  $SO_2$  values in tissues presenting extreme  $pO_2$  values (very high or very low). Accordingly, at the intra-tumoral level, we observed a general higher fraction of voxels with  $\Delta R_1 > 0$  in 9 L-gliomas than in rhabdomyosarcomas (Figure 4). Yet we also noticed that ITPP induced a higher fraction of voxels presenting a  $\Delta R_2^* > 0$  in rhabdomyosarcomas (Figure 4).

This raises the question as to whether  $R_2^*$  could be used to monitor the change in tumor  $pO_2$  induced by an allosteric effector of Hb. In two studies using a different allosteric effector of Hb, RSR13, similar changes in  $R_2^*$  were not observed. In the study of Kelly et al,<sup>32</sup> RSR13 induced an increase in BOLD signal intensity (meaning a decrease in  $R_2^*$ ) in NCI-H460 human lung carcinoma xenograft. By contrast, in the work of Hou et al,<sup>39</sup> RSR13 had scarcely any effect on the  $R_2^*$  signal in RIF-1 tumors. It should be noted that both ITPP and RSR13 significantly enhanced tumor  $pO_2$  in the models under study.<sup>27,32</sup> Figure 9 presents a model that may explain the complexity in  $R_2^*$  signal changes.  $R_2^*$  is sensitive to the change in [dHb]. In the three situations illustrated, (A), (B) and (C), the allosteric effector significantly increases tumor  $pO_2$ . Yet the changes in [dHb] do not follow the change in  $pO_2$ , as Hb saturation can increase, decrease or remain stable. Thus  $R_2^*$  is not suitable for monitoring the change in  $pO_2$  in response to allosteric modifiers of Hb: if the allosteric effector does not induce any change in tumor blood flow or blood volume, but only induces change in the ODC, the saturation of hemoglobin should be determined by the new corresponding  $pO_2$  value (Figure 9) on the

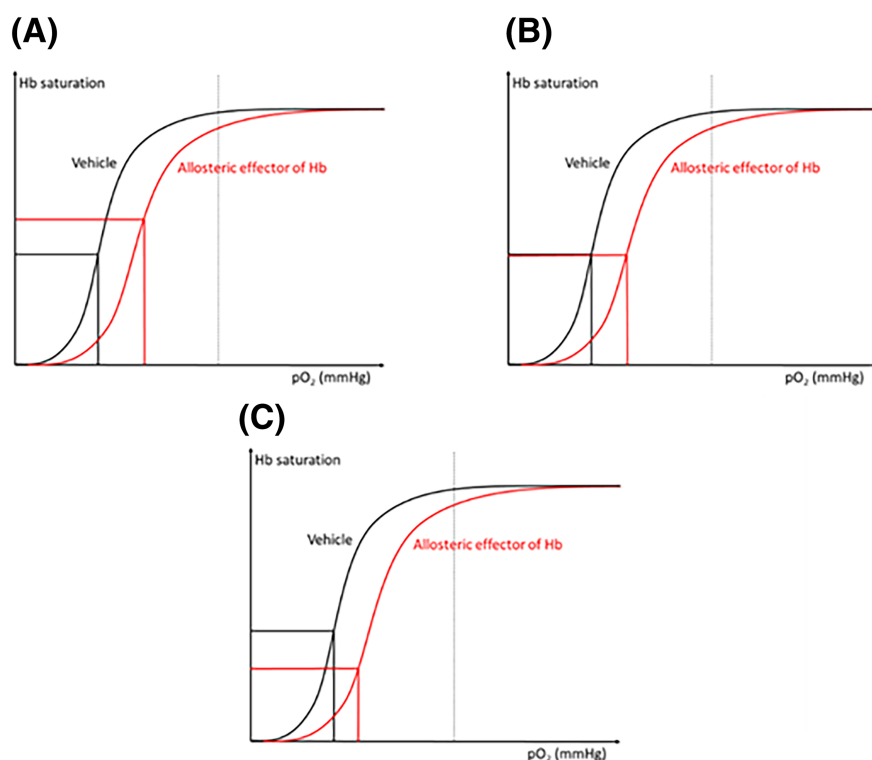


**FIGURE 9** The complexity of  $R_2^*$  under the effect of an allosteric effector of hemoglobin. Note that if there is no change in the blood flow or blood volume, an increase in the degree of hemoglobin saturation (which means a decrease in the proportion of dHb) leads to a decrease in  $R_2^*$  and vice versa. (A), (B) and (C) illustrate three possibilities of  $R_2^*$  if the allosteric effector induces a shift in the oxygen dissociation curve (ODC) and an enhancement in tumor  $pO_2$ . The change in  $R_2^*$  depends on the degree of Hb saturation but not on the real tumor  $pO_2$



new ODC. Note that the equilibrium of  $pO_2$  after treatment depends on many factors, including tumor type and the impact of the drug on the metabolic rate or on the oxygen consumption rate of tumor cells. The mechanism of OCR modulators can be complex and usually includes the change in tumor perfusion or in tumor metabolic activity.<sup>35,37</sup> These factors are unrelated to the real change in tumor  $pO_2$  and can modify the  $R_2^*$  signal, hindering interpretation of the results. In brief, caution should be exercised when interpreting  $R_2^*$  as the marker reflects the concentration of dHb per volume, but not oxygenation per se.

In the study of Fylaktakidou et al.,<sup>20</sup> ITPP was found to be a powerful allosteric effector of Hb. The incubation of ITPP with the human whole blood sample showed that the compound was able to increase the P50 of the blood by up to 40% (P50 = partial pressure of oxygen under which 50% of Hb is saturated with  $O_2$ ). The ability of ITPP to induce the P50-shift in a sample of human blood was dose-dependent and reached a maximum at a concentration of 60mM. At a dose of 30mM, ITPP induced a 36% P50-shift and the Hill coefficient went from 2.4 to 1.6. Interestingly, ITPP appears to induce a stronger effect on P50-shift in murine blood samples than in human blood samples: at 4mM, ITPP induced a 30% P50-shift in a murine blood sample versus a less than 3% P50-shift in a human blood sample. These in vitro findings could explain the large decrease in hemoglobin saturation that we observed in this study (Figure 6).

It should be noted that, despite the significant improvement in tumor  $pO_2$  in both tumor models, 9 L-glioma and rhabdomyosarcoma, ITPP in monotherapy or combined with radiation therapy did not improve the treatment outcome in the tumor models under study.<sup>29</sup> Besides tumor oxygenation, other factors can contribute to the radiosensitivity of cancer cells, such as the ability to repair DNA damage and cancer cell repopulation following irradiation. In particular, the findings showed that ITPP may be involved in the PI3K pathway, which is a key regulator of various cellular functions, from cell proliferation to cell survival, and is implicated in all major mechanisms of radioresistance.

In conclusion, ITPP was able to increase tumor  $pO_2$  in a rhabdomyosarcoma and a 9 L-glioma model. The value of the MRI biomarkers  $R_1$  and  $R_2^*$  was increased by ITPP treatment. The interpretation of the results needs to take into account that  $R_1$  and  $R_2^*$  can be biased by multiple factors, unrelated to changes in  $pO_2$ . In this study, we identified that the acute effect of ITPP on tumor  $pO_2$  was the result of a combination of right-shifting of the ODC, a decrease in pH and a decrease in OCR. In addition, we concluded that  $R_2^*$  is not suitable to monitor change in tumor  $pO_2$  induced by an allosteric effector of Hb.

## ACKNOWLEDGEMENTS

This study was supported by grants from the Belgian National Fund for Scientific Research (FNRS) and the Fournier-Majoie Foundation. BFJ is Senior Research Associate of the FNRS.

## ORCID

Bernard Gallez  <https://orcid.org/0000-0002-5708-1302>

Bénédicte F. Jordan  <https://orcid.org/0000-0002-7126-2206>

## REFERENCES

1. Vaupel P, Mayer A. Tumor Hypoxia: Causative Mechanisms, Microregional Heterogeneities, and the Role of Tissue-Based Hypoxia Markers. In: Luo Q, Li LZ, Harrison DK, Shi H, Bruley DF, eds. *Oxygen Transport to Tissue XXXVIII*. Vol. 923 Cham: Springer International Publishing; 2016:77-86.
2. Overgaard J. Hypoxic radiosensitization: adored and ignored. *J Clin Oncol*. 2007;25:4066-4074.
3. Jordan BF, Cron GO, Gallez B. Rapid monitoring of oxygenation by  $^{19}F$  magnetic resonance imaging: Simultaneous comparison with fluorescence quenching. *Magn Reson Med*. 2009;61:634-638.
4. Gallez B, Baudalet C, Jordan BF. Assessment of tumor oxygenation by electron paramagnetic resonance: principles and applications. *NMR Biomed*. 2004;17:240-262.
5. Kodibagkar VD, Wang X, Pacheco-Torres J, Gulaka P, Mason RP. Proton imaging of siloxanes to map tissue oxygenation levels (PISTOL): a tool for quantitative tissue oximetry. *NMR Biomed*. 2008;21:899-907.
6. Tran L-B-A, Bol A, Labar D, et al. Hypoxia imaging with the nitroimidazole  $^{18}F$ -FAZA PET tracer: A comparison with OxyLite, EPR oximetry and  $^{19}F$ -MRI relaxometry. *Radiother Oncol*. 2012;105:29-35.
7. Wolf G, Abolmaali N. Preclinical molecular imaging using PET and MRI. *Recent Results Cancer Res*. 2013;187:257-310.
8. Dewhirst MW, Klitzman B, Braun RD, Brizel DM, Haroon ZA, Secomb TW. Review of methods used to study oxygen transport at the microcirculatory level. *Int J Cancer*. 2000;90:237-255.
9. Gu Y, Bourke VA, Kim JG, Constantinescu A, Mason RP, Liu H. Dynamic response of breast tumor oxygenation to hyperoxic respiratory challenge monitored with three oxygen-sensitive parameters. *Appl Optics*. 2003;42:2960-2967.
10. O'Connor JPB, Robinson SP, Waterton JC. Imaging tumour hypoxia with oxygen-enhanced MRI and BOLD MRI. *Br J Radiol*. 2019 Mar;92(1095):20180642. <https://doi.org/10.1259/bjr.20180642> Epub 2019 Jan 24.
11. O'Connor JPB, Naish JH, Jackson A, et al. Comparison of normal tissue  $R_1$  and  $R_2^*$  modulation by oxygen and carbogen. *Magn Reson Med*. 2009;61:75-83.
12. Burrell JS, Walker-Samuel S, Baker LCJ, et al. Exploring  $\Delta R_2^*$  and  $\Delta R_1$  as imaging biomarkers of tumor oxygenation. *J Magn Reson Imaging*. 2013;38:429-434.

13. O'Connor JPB, Boulton JKR, Jamin Y, et al. Oxygen-enhanced MRI accurately identifies, quantifies, and maps tumor hypoxia in preclinical cancer models. *Cancer Res.* 2016;76:787-795.
14. Hallac RR, Zhou H, Pidikiti R, et al. Correlations of noninvasive BOLD and TOLD MRI with pO<sub>2</sub> and relevance to tumor radiation response. *Magn Reson Med.* 2014;71:1863-1873.
15. Cao-Pham T-T, Joudiou N, Van Hul M, et al. Combined endogenous MR biomarkers to predict basal tumor oxygenation and response to hyperoxic challenge. *NMR Biomed.* 2017;30(12). <https://doi.org/10.1002/nbm.3836>
16. Cao-Pham T-T, Tran L-B-A, Collier F, et al. Monitoring tumor response to carbogen breathing by oxygen-sensitive magnetic resonance parameters to predict the outcome of radiation therapy: a preclinical study. *Int J Radiat Oncol Biol Phys.* 2016;96:149-160.
17. Jordan BF, Magat J, Collier F, et al. Mapping of oxygen by imaging lipids relaxation enhancement: a potential sensitive endogenous MRI contrast to map variations in tissue oxygenation. *Magn Reson Med.* 2013;70:732-744.
18. Suh JH. Efaproxiral: a novel radiation sensitizer. *Expert Opin Investig Drugs.* 2004;13:543-550.
19. Suh JH, Stea B, Tankel K, et al. Results of the phase III ENRICH (RT-016) study of Efaproxiral administered concurrent with whole brain radiation therapy (WBRT) in women with brain metastases from breast cancer. *Int J Radiat Oncol Biol Phys.* 2008;72:S50-S51.
20. Limani P, Linecker M, Kron P. Development of OXY111A, a novel hypoxia-modifier as a potential antitumor agent in patients with hepato-pancreato-biliary neoplasms - protocol of a first Ib/IIa clinical trial. *BMC Cancer.* 2016;16:812-818.
21. Fylaktakidou KC, Lehn J-M, Greferath R, Nicolau C. Inositol tripyrophosphate: a new membrane permeant allosteric effector of haemoglobin. *Bioorg Med Chem Lett.* 2005;15:1605-1608.
22. Duarte CD, Greferath R, Nicolau C, Lehn J-M. Myo-inositol trispyrophosphate: a novel allosteric effector of hemoglobin with high permeation selectivity across the red blood cell plasma membrane. *Chembiochem.* 2010;11:2543-2548.
23. Kieda C, Hafny-Rahbi BE, Collet G, et al. Stable tumor vessel normalization with pO<sub>2</sub> increase and endothelial PTEN activation by inositol trispyrophosphate brings novel tumor treatment. *J Mol Med.* 2013;91:883-899.
24. Raykov Z, Grekova SP, Bour G, et al. Myo-inositol trispyrophosphate-mediated hypoxia reversion controls pancreatic cancer in rodents and enhances gemcitabine efficacy. *Int J Cancer.* 2014;134:2572-2582.
25. Aprahamian M, Bour G, Akladios CY, et al. Myo-InositolTrisPyroPhosphate treatment leads to HIF-1 $\alpha$  suppression and eradication of early hepatoma tumors in rats. *Chembiochem.* 2011;12:777-783.
26. Jordan BF, Baudelet C, Gallez B. Carbon-centered radicals as oxygen sensors for in vivo electron paramagnetic resonance: screening for an optimal probe among commercially available charcoals. *MAGMA.* 1998;7(2):121-129.
27. Crockart N, Jordan BF, Baudelet C, et al. Glucocorticoids modulate tumor radiation response through a decrease in tumor oxygen consumption. *Clin Cancer Res.* 2007;13:630-635.
28. Ansiaux R, Baudelet C, Jordan BF, et al. Mechanism of reoxygenation after antiangiogenic therapy using SU5416 and its importance for guiding combined antitumor therapy. *Cancer Res.* 2006;66:9698-9704.
29. Jordan BF, Grégoire V, Demeure RJ, et al. Insulin increases the sensitivity of tumors to irradiation: involvement of an increase in tumor oxygenation mediated by a nitric oxide-dependent decrease of the tumor cells oxygen consumption. *Cancer Res.* 2002;62:3555-3561.
30. Tran LBA, Cao-Pham TT, Jordan BF, Deschoemaeker S, Heyerick A, Gallez B. Impact of myo-inositol trispyrophosphate (ITPP) on tumour oxygenation and response to irradiation in rodent tumour models. *J Cell Mol Med.* 2019;23(3):1908-1916.
31. FöRnvik K, Zolfaghari S, Salford LG, Redebrandt HN. ITPP treatment of RG2 glioblastoma in a rat model. *Anticancer Res.* 2016;36:5751-5756.
32. Kelly CJ, Hussien K, Fokas E, et al. Regulation of O<sub>2</sub> consumption by the PI3K and mTOR pathways contributes to tumor hypoxia. *Radiother Oncol.* 2014;111:72-80.
33. Li C, Li Y, He L, et al. PI3K/AKT signaling regulates bioenergetics in immortalized hepatocytes. *Free Radic Biol Med.* 2013;60:29-40.
34. Blockley NP, Jiang L, Gardener AG, Ludman CN, Francis ST, Gowland PA. Field strength dependence of R<sub>1</sub> and R<sub>2</sub><sup>\*</sup> relaxivities of human whole blood to proance, vasovist, and deoxyhemoglobin. *Magn Reson Med.* 2008;60:1313-1320.
35. Howe FA, Robinson SP, Rodrigues LM, Griffiths JR. Flow and oxygenation dependent (FLOOD) contrast MR imaging to monitor the response of rat tumors to carbogen breathing. *Magn Reson Imaging.* 1999;17:1307-1318.
36. Jordan BF, Crockart N, Baudelet C, Cron GO, Ansiaux R, Gallez B. Complex relationship between changes in oxygenation status and changes in R<sub>2</sub><sup>\*</sup>: the case of insulin and NS-398, two inhibitors of oxygen consumption. *Magn Reson Med.* 2006;56:637-643.
37. Little RA, Jamin Y, Boulton JKR, et al. Mapping hypoxia in renal carcinoma with oxygen-enhanced MRI: comparison with intrinsic susceptibility MRI and pathology. *Radiology.* 2018;288:739-747.
38. Jordan BF, Misson P, Demeure R, Baudelet C, Beghein N, Gallez B. Changes in tumor oxygenation/perfusion induced by the NO donor, isosorbide dinitrate, in comparison with carbogen: monitoring by EPR and MRI. *Int J Radiat Oncol Biol Phys.* 2000;48:565-570.
39. Hou H, Khan N, O'Hara JA, et al. Effect of RSR13, an allosteric hemoglobin modifier, on oxygenation in murine tumors: an in vivo electron paramagnetic resonance oximetry and BOLD MRI study. *Int J Radiat Oncol Biol Phys.* 2004;59:834-843.

**How to cite this article:** Cao-Pham T-T, Tran-Ly-Binh A, Heyerick A, et al. Combined endogenous MR biomarkers to assess changes in tumor oxygenation induced by an allosteric effector of hemoglobin. *NMR in Biomedicine.* 2020;33:e4181. <https://doi.org/10.1002/nbm.4181>